MARINE & FRESHWATER RESEARCH

Linking patterns of freshwater discharge and sources of organic matter within the Río de la Plata estuary and adjacent marshes

Journal:	*Marine and Freshwater Research*
Manuscript ID	MF16286.R1
Manuscript Type:	Research paper
Date Submitted by the Author:	n/a
Complete List of Authors:	Bergamino, Leandro; Centro Universitario Regional Este (CURE), Universidad de la República Schuerch, Mark ; University of Cambridge, Department of Geography, Cambridge Coastal Research Unit, Cambridge, UK. Tudurí, Adriana; Universidad de la República, Facultad de Ciencias, Sección Oceanología Carretero, Silvina ; Consejo Nacional de Investigaciones Científicas y Técnicas (CONICET), Facultad de Ciencias Naturales y Museo, Universidad Nacional de La Plata Garcia-Rodriguez, Felipe; Centro Universitario Regional Este (CURE), Universidad de la República
Keyword:	estuarine, organic matter, stable isotopes, sedimentation, hydrology

Linking patterns of freshwater discharge and sources of organic matter within the Río de la Plata estuary and adjacent marshes

Leandro Bergamino[1], Mark Schuerch[2], Adriana Tudurí[3], Silvina Carretero[4], Felipe García-Rodríguez[1]

[1] Centro Universitario Regional Este (CURE), Universidad de la República, Rutas 9 y 15 s/n, Rocha, Uruguay

[2] University of Cambridge, Department of Geography, Cambridge Coastal Research Unit, Cambridge, UK.

[3] Universidad de la República, Facultad de Ciencias, Sección Oceanología, Iguá 4225, Montevideo 11400, Uruguay.

[4] Consejo Nacional de Investigaciones Científicas y Técnicas (CONICET), Facultad de Ciencias Naturales y Museo, Universidad Nacional de La Plata (UNLP), 64 no. 3, 1900 La Plata, Argentina

Corresponding Author: Leandro Bergamino. E-mail: lbergamino@gmail.com

Abstract

We investigated carbon isotopic ratios $\delta^{13}C$ vs. C/N for surface sediments throughout a large estuarine system (Río de la Plata, RdlP), combined with sediment cores from adjacent marshes to infer main carbon sources. We also evaluated the influence of the El Niño-Southern Oscillation (ENSO) and associated high freshwater discharge events on the organic matter transport within the estuary. The isotopic pattern in surface sediments of the RdlP showed the upper reaches to be influenced by riverine particulate matter ($\delta^{13}C$ range -24 to -26‰). Similarly, in the sediment cores from marshes of the upper reaches, $\delta^{13}C$ values decreased from -24‰ in ancient sediments to -28‰ in recent sediments reflecting an increased contribution of organic matter from land including C3 plants and freshwater phytoplankton during the last 50 years. However, the lower reaches represent a depositional environment of marine algae ($\delta^{13}C$ ranged -21 to -23‰), with no influence of detritus from adjacent marshes indicating minor erosion of the marshes in the lower reaches operating as carbon sink habitats. Our isotopic analysis point that the transport and deposition of terrigenous organic matter within the RdlP and adjacent marsh habitat appear to be both temporally and spatially linked to hydrology patterns.

Additional keywords: Carbon isotopes; C/N ratios; marsh; estuarine sediments; Río de la Plata.

Introduction

Estuaries are characterized by gradients of physical, chemical and biological variables including salinity, nutrients and primary productivity (Whitfield and Elliott 2011). Due to high nutrient loads from river discharge and the diversity of organic matter sources such as zoo/phytoplankton, microphytobenthos, macrophytes, bacteria, estuaries have long been recognized as highly productive habitats (Paerl 2006). Furthermore, the interactions between aquatic and adjacent terrestrial ecosystems through the flow and exchange of organic matter are increasingly apparent (Nakano and Murakami 2001; Cole *et al*. 2011). Such allochthonous resources can significantly subsidize ecosystems of low productivity and influence population dynamics (Polis *et al*. 1997; Pace *et al.* 2004; Abrantes *et al.* 2013), and secondary production (Valiela and Bartholomew 2015). In particular, marsh areas are frequently coupled to adjacent aquatic ecosystems, such as estuaries, by contributing with organic matter exports (Abrantes and Sheaves 2008; Whitfield and Elliott 2011). Therefore, the import of terrestrial organic matter into estuarine systems is critical to reliably assess both ecosystem functioning and productivity (Abrantes *et al.* 2013).

The continental freshwater input of large estuaries into the ocean is commonly modulated by climatic forcing (Piola *et al.* 2008; Barreiro 2010; García-Rodríguez *et al.* 2014). In particular, an important characteristic of aquatic systems in South America is the variability associated with the El Niño-Southern-Oscillation (ENSO) events (a recurring 2–7 year cycle of coupled ocean–atmosphere dynamics in the equatorial Pacific) and rainfall patterns (Mechoso and Perez-Iribarren 1992; Depetris *et al.* 1996; Barreiro 2010). Strong ENSO influence occurs during warm-phase ENSO events that are associated with increased rainfall events over southeastern

South America (Barreiro, 2010), leading to high discharge events in the Uruguay/Paraná River (Bischoff *et al.* 2000; Camilloni and Barros 2000). In estuarine ecosystems, such periods of high discharge can considerable modify the concentrations of material and nutrients transferred between ecosystems (Goñi *et al.* 2009; Valiela and Bartholomew 2015). Hence, studying both modern and historical sources of organic matter from the continental and fluvial to the transitional estuarine region and the adjacent ocean, is important to infer the transport and budgets of organic matter in relation to hydrological and oceanographic processes (e.g. Burone *et al.* 2013).

Stable carbon isotope composition ($\delta^{13}C$) together with C/N ratios of bulk sedimentary organic matter have been successfully used to infer the relative influence of marine vs. terrestrial sources in coastal environments (e.g. Müller and Voss 1999; Malamud-Roam and Ingram 2001; Tue *et al.* 2011; Remeikaitė-Nikienė *et al.* 2016). This is because $\delta^{13}C$ values are usually minimally affected by diagenetic processes in sediment organic matter (Thornton and McManus 1994; Lautenschlager *et al.* 2014). Terrestrial material from C3 pathways exhibits $\delta^{13}C$ values that range between -32 and -21‰. On the other hand, C4 plants typically show $\delta^{13}C$ values between -17 to -9‰, while marine organic matter typically displays $\delta^{13}C$ values between -24 to -18‰ (Meyers 1994; Lamb *et al.* 2006). Furthermore, terrestrial vegetation has relatively high C/N ratios, usually higher than 12, due to the lignin and cellulose abundance, but C/N ratios from 4 to 10 are characteristic for marine organic substances (Meyers 1994, 2003). In this context, distinctive suits of C/N and $\delta^{13}C$ values characteristics of C3, C4 plants, marine, and freshwater algae can be used to identify major sources of organic matter in coastal sediments (Lamb *et al.* 2006; Tue *et al.* 2011; Remeikaitė-Nikienė *et al.* 2016).

Some studies (Botto *et al.* 2011; Burone *et al.* 2013) have applied stable isotope analysis in surface sediments within the Río de la Plata (RdlP) answering the question of the origin of organic matter (i.e. terrigenous or marine), but investigations on land-water coupling including the adjacent marshes of the RdlP are less common. Therefore, the aim of this study was to gain insight into the sources and distribution of organic matter within the RdlP to infer both the mechanisms and factors responsible for variations in organic matter material fluxes. We assessed $\delta^{13}C$ values and C/N ratios in both sediment cores and surface sediment samples along a salinity gradient to assess the spatial patterns in the sources of organic matter (from riverine and terrestrial plant material to marine phytoplankton). In addition, we explored the temporal pattern related to river discharge variability associated with ENSO events. We hypothesized that different patterns of freshwater discharge associated with ENSO events induce a change in the sources of organic matter deposited within the RdlP estuary and the fringing marshes.

Materials and methods

Study area

The study area comprises the inner, middle and outer regions of the RdlP estuary (34°10′–36°20′ S and 55°00′–58°30′ W) and the adjacent marsh habitats (Fig. 1). This estuary region represents a highly productive area that sustains valuable artisanal and coastal fisheries in Uruguay and Argentina (FREPLATA 2004). The RdlP estuary is one of the world's largest estuaries, with an average annual river discharge of ca. 24,000 m^3 s^{-1} representing a confluence of the Paraná and Uruguay River with a mixohaline area of 38,000 km^2 (Mianzan *et al.* 2001). The estuary is

116 approximately 320 km in length and 250 km in width (minimum of 40 km). It is relatively
117 shallow with only 5-15 m of water depth, and the tide range is small, averaging about 0.60 m
118 (Framiñan and Brown, 1996). River discharge increases from April to June with a sharp rise in
119 May. It reaches minimum values from December to March (Guerrero *et al.* 1997). Salinity varies
120 significantly during the year in negative correlation with river runoff; lowest salinities are found
121 during periods of high river discharge from April to August, and highest salinities are observed
122 in December and January (Guerrero *et al.* 1997). The estuary can be divided into three sections
123 based on its morphology, and the prevailing hydrodynamics (Framiñan and Brown 1996; Nagy *et*
124 *al.* 2002). The upper reaches are characterized by freshwater conditions and water column depths
125 lower than 5 m (Mianzan *et al.* 2001; Nagy *et al.* 2002). The middle reaches are characterized by
126 the salt intrusion boundary, prevailing shallow waters and intermediate channels (<10 m). A
127 submersed bar, called Barra del Indio shoal, is a sedimentary facies consequent of the bottom
128 salinity front and represent the boundary between the riverine regime and the salt wedge regime,
129 following approximately, the 10 m isobath (Guerrero *et al*. 1997; Fig. 1). The lower reaches with
130 maritime channel (10-20 m depth), reflect a gradual increase in the marine influence including a
131 small transitional section together with the marine part of the estuary with a characteristic
132 salinity and seston gradient (Calliari *et al*. 2005). Here, the Subtropical Convergence emerges
133 where the southward-flowing Brazil Current meets the northward-flowing Malvinas (Falkland)
134 Current, resulting in complex frontal systems and hydrographic structures like eddies and
135 meanders (Calliari *et al.* 2009). The average annual suspended sediment load from the Paraná
136 and Uruguay rivers is 79.8 x 10^6 tons yr^{-1}, and is characterized by 75% coarse to medium silt,
137 15% fine to very fine silt, and 10% clay (Giberto *et al.* 2004).
138

Large parts of the estuary are fringed by freshwater and salt marshes, whereas the salt marshes along the Uruguayan coast are dominated by halophytes including *Spartina montevidensis* (C4), *S. longispina* (C4), *Juncus acutus* (C3) and *Salicornia ambigua* (Mianzan *et al.* 2001). Along the Argentinean coast, marshes of the Samborombón bay are dominated by the cordgrasses *Spartina alterniflora* (C4), *Spartina densiflora* (C4) and *Sarcocornia perennis* (C3) (Isacch *et al.* 2006). Meanwhile, the freshwater marshes in the inner estuary are dominated by small emergent plants including *Ludwigia* spp., *Alternanthera philoxeroides, Echinodorus* sp., *Eryngium sp.*

Data collection

Monthly average values of the Paraná and Uruguay rivers discharge were obtained from the Integrated Hydrologic Database (http://bdhi.hidricosargentina.gov.ar/sitioweb/frmInicial.aspx) by the Secretary of Water Resources, Argentina. Stations representing the Paraná and the Uruguay River are "Túnel subfluvial'' and "Paso de los Libres'', respectively. Relative anomalies of river discharge are shown in Fig. 2, calculated following Piovano *et al.* (2004) as: Anomaly $Q=(Qi - Qaverage)/Qaverage$, where Qi is the sum of the monthly discharge averages per year and $Qaverage$ is the average of all values of the time series (i.e. 1909 AD-present). In specific years such as 1982/1983, and 1997/1998 the Paraná and Uruguay rivers experienced high river discharges, which were greater than two times the annual mean of 24,000 m^3 s^{-1}. Furthermore, during the period 2000/2001 only the Uruguayan river showed increased mean river discharge, and during the years 1991/1992 only the Paraná river discharges were twice its average (Fig. 2). These anomalies coincide with strong El Niño events according to the Oceanic Niño Index (ONI, http://www.cpc.ncep.noaa.gov/products/analysis_monitoring/ensostuff/ensoyears.shtml). The

ONI is defined as a three month running mean of sea surface temperature (SST) anomalies in the Niño 3.4 region (5°N–5°S latitude, 120°W–170°W longitude), with values greater than +(-)1.5ºC indicating strong El Niño (La Niña) conditions.

Sampling and stable isotope analysis

The data of six sediment cores that were collected in marsh sites adjacent to the RdlP by Schuerch *et al.* (2016) were used for the present analysis (Fig. 1). Coring locations were in the inter- and supratidal zones of the marshes (above the mean high water level) and characterized by dense vegetation cover, in order to avoid a stress caused by currents and waves. Except for core 08-1, all cores were collected on the river banks of the RdlP. Coring site 08-1 was located about 900 m from the RldP in the river mouth of the Río Salado. Cores were extracted using PVC tubes with an inner diameter of 10.3 cm. Core lengths ranged from 51 to 115 cm, averaging 91.5 cm. Cores were sliced into layers of 2 cm for all depths between 0 and 20 cm, 3 cm for depths between 20 and 50 cm and 5 cm for all layers below (Schuerch *et al.* 2016). For core 12-1 and 10-1 a total of 21 and 24 sediment samples were collected respectively. A total of 21 sediment samples were collected from core 19-1, 26 samples for the core 09-1, 25 samples for the core 08-1, and 22 for the core 02-1.

The sediment samples were dried at 60°C until constant weight and manually ground to a fine homogeneous powder using mortar and pestle. Elemental and bulk isotope analysis was conducted by the element analyzer "NA1110" (CE Instruments, Rodano, Italy) and the mass spectrometer "Delta Plus" coupled via a "Conflo III" (Werner *et al.* 1999).

Surface sediments samples were collected from 25 stations within the RdlP estuary during 1-2 weeks cruises (FREPLATA-Ifremer research) in March (warm season) and June (cold season) 2010. Sampling stations were located in the upper, middle and lower reaches of the estuary (Fig. 1). Sediments samples were collected using a Van Veen grab. This approach has also been used in previous studies of biochemical composition in surficial sediments (e.g. García-Rodríguez *et al.* 2014). In the laboratory, samples were acid washed (3 h in 10% HCl) to remove carbonates, rinsed in distilled water and then dried again for 24 h at 60 °C. All sediment samples were ground to a fine homogeneous powder using mortar and pestle for elemental (C_{org}, N_{total}) and bulk isotope analyses, including the measurement of $\delta^{13}C$ ratios. All samples were then analyzed using a Thermo Finnigan Flash EA 1112 series elemental analyzer equipped with a Thermo Finnigan Delta Plus XP isotope ratio mass spectrometer by the *Centro de Aplicaciones de Tecnología Nuclear en Agricultura Sostenible*, University of Uruguay.

Spatial changes of the $\delta^{13}C$ and C/N ratios for the marsh cores and surface sediments were determined by non-metric multi-dimensional scaling plots (nMDS: Kruskal and Wish 1978) using the software Paleontological Statistics (PAST) 1.42 (Hammer *et al.* 2001). For this purpose, similarity matrices were constructed on normalized data (by subtracting the mean from each datapoint and dividing by the standard deviation) using the Euclidean distance similarity measure. Analyses of similarities (ANOSIM with 1000 permutation) were performed on each Euclidean similarity matrix to determine resemblance in $\delta^{13}C$ and C/N ratios among sites within the RdlP and adjacent marsh sites. For the marsh cores we included all dates/depths available, and for the superficial estuary sediment data of both sampling periods (March and June) were included into this analysis.

208

209 *Sample dating*

210 Radionuclide analysis (^{210}Pb and ^{137}Cs) was conducted by Schuerch *et al.* (2016) in order to
211 determine the years of deposition for each of the sediment layers. Alpha spectrometry, using an
212 *Ortec Octête Plus* alpha-spectrometer, was applied to determine sediment ages of the cores 02-1,
213 12-1 and 19-1. Prior to the analysis, the sediment samples were digested in the presence of ^{209}Po
214 yield tracer and by means of 3 ml HF, 5 ml HNO_3, 2 ml HCL. Digestion was accelerated by
215 heating the samples with a *MARS 6* microwave system, followed by the spontaneous deposition
216 of polonium on silver disks and the measurement of the resulting ^{209}Po activity. Reference
217 samples for validation purposes were conducted using uranium reference material *UREM-11*.

218

219 Gamma spectrometry, using high-purity germanium detectors (*CANBERRA BE3830P*), was
220 employed for age-dating of the cores 08-1 and 10-1 (for details see Schuerch *et al.* 2016).
221 Aliquots of 10-15 g were, therefore, placed in sealed vials and allowed to sit for three weeks
222 until equilibrium has established between ^{226}Ra and ^{214}Bi. ^{210}Pb, ^{214}Pb, ^{214}Bi and ^{137}Cs were
223 measured via their gamma peaks at 45.6 KeV, 352 KeV, 609 KeV, and 661 KeV, respectively.
224 Unsupported ^{210}Pb, needed for dating purposes, was calculated as the difference between the
225 total ^{210}Pb and the ^{226}Ra intensity. ^{226}Ra, in turn, was calculated as the mean value of ^{214}Bi and
226 ^{214}Pb, both of which were assumed to be in equilibrium with ^{226}Ra.

227

228 Based on the unsupported ^{210}Pb activities (see supplementary material), sediment ages were
229 derived by means of the *Constant-Flux* (CF), or *Constant-rate of supply* (CRS), dating model in
230 combination with the *Constant Flux Constant Sedimentation* (CFCS) model, where the captured

^{210}Pb inventory was incomplete (Appleby and Oldfield 1978; Sanchez-Cabeza and Ruiz-Fernández 2012; Schuerch *et al.* 2016).

Results

δ^{13}C, and C/N from marsh sites

The δ^{13}C ratios for the cores 12-1 and 10-1, located in the Paraná Delta near the freshwater discharge in the upper reaches, showed a considerable range of δ^{13}C values between -23.2 and -28.3‰ (Fig. 3). Downcore sediment samples from the two cores in the upper reaches of the estuary displayed higher δ^{13}C ratios with an upward-decreasing trend that is more pronounced in core 10-1 as compared to core 12-1. Sediments showed minimum δ^{13}C ratios of -28.3‰ in core 12-1 (in a depth of 5 cm) and -27.7‰ in core 10-1 (in a depth of 5 cm). In sediments from core 10-1, δ^{13}C values particularly sharply decreased during the extreme ENSO events of 1982/1983, 1997/1998 and 2000/2001. In the core 12-1, δ^{13}C decreased abruptly during 2000/2001 below -27‰. Furthermore, C/N ratios of sedimentary organic matter in the upper reaches of the estuary were generally higher than 9, and ranged between 9 and 13 (Fig. 3). The C/N ratios in core 10-1 increased abruptly above 10 during the extreme ENSO event of 1997/1998, whereas in core 12-1, located in vicinity of Uruguay river, the amplitude of the ENSO related peaks in C/N ratios are less pronounced (e.g. the 2000/2001 ENSO event). Similar to the abrupt δ^{13}C decrease after the 2000/2001 ENSO, the C/N ratios in core 12-1 show a remarkable drop.

Over the length of the four cores from the lower reaches of the estuary (cores 19-1, 08-1, 09-1 and 02-1), δ^{13}C values showed a range of 8.6‰, i.e. between -10.4 and -19.0‰ (Fig. 4a, b, e). In

sediments from the core located furthest away from the freshwater discharge (core 19-1), $\delta^{13}C$ showed minimum values in the years 1986/1987, 1993/1994, and 1997/1998 with -17.9, -17.5, and -17.6‰ respectively. The C/N ratios equal to zero in the upper section of core 19-1 can be explained as a consequence of the possible loss of organic carbon derived from decomposition of organic matter and remineralization that introduces uncertainty to infer organic matter (Müller 1977; Meyers 1997; Sampei and Matsumoto 2001). $\delta^{13}C$ values in sediments from core 08-1 in the lower reaches decrease abruptly after the ENSO events of 1982/1983 and 1992/1993 below -18‰. Simultaneously, C/N ratios drop below 12 and 10 respectively (Fig. 4d). For the core 09-1 isotopic values of $\delta^{13}C$ reach their minimum of -17.8 and -17.6‰ in sediments at 70 and 50 cm depth respectively (Fig. 4e). For this core, no dating is available hence isotopic patterns are analyzed as a function of depth only (Fig. 4e,g). Maximum $\delta^{13}C$ values together with highest C/N ratios of -9‰ and 22, respectively were detected in sediments in about 6 cm depth. In the marsh core 02-1, located in the lower reaches of the RdlP along the Uruguayan coast, $\delta^{13}C$ ranged between -19.5 and -16.8‰ and tended to increase from 1960 to present days (Fig. 4f).

Analysis of the marsh cores from the upper reaches (core 12-1 and 10-1) indicated that organic matter is composed of a mixture of freshwater algae and terrestrial C3 plants (core 10-1: range of $\delta^{13}C$ between -25.5 and -27.6‰, range of C/N between 10.4 and 12.3; core 12-1: range of $\delta^{13}C$ between -28.5 and -25.6‰, range of C/N ratio between 9.6 and 13.3, Fig. 5). On the other hand, $\delta^{13}C$ and C/N values of sediment cores from saltmarshes located in the lower reaches were associated with a mixture of marine algae and C4 marsh grasses (Fig. 5).

$\delta^{13}C$, and C/N of surface samples within the RdlP

The $\delta^{13}C$ values for surface sediments in collected during the cold season showed a narrower range than the $\delta^{13}C$ values of the samples collected during the warm season (-20.2 to -24.6‰ and -21.2 to 26.2‰ respectively). $\delta^{13}C$ values showed a clear trend along the estuarine gradient with sediments from the upper reaches having the most depleted carbon (-25 to -26‰; Fig. 6), while such values progressively increased towards the middle and lower reaches (Fig. 6). The C/N ratios in surface sediments within the RdlP showed little difference between seasons with values ranging from 6.6 to 8.9 for samples collected in March and from 6.5 to 8.9 in for the samples collected in June. The variability of C/N ratios among the sites also appears to be small (Fig. 6).

Based on the $\delta^{13}C$ values and C/N ratios, the marsh core data were grouped in nMDS plots (all depths pooled Fig. 7a), while being separated from surface sediment samples from the upper, middle and lower reaches of the RdlP (Fig. 7b), . In both cases samples from the middle reaches spread between the upper and lower reaches groups. Not only the stress values (< 0.1) indicated a significant two-dimensional representation of the groups, but also the ANOSIM results revealed significant differences in the isotopic composition among all surface samples within the RdlP (R =0.83, P = 0.0001) and among the different marsh sites (R = 0.58, P = 0.0001). Furthermore, the nMDS plot on $\delta^{13}C$ values and C/N ratios including all sediment samples (core data and surface sediments) showed different distribution patterns and a clear separation between marsh and estuarine sites (Fig. 7c).

Discussion

Our isotopic data highlighted differential composition and organic matter along the RdlP and adjacent marshes, suggesting different sources. The isotopic measurements in marsh sediments from the upper reaches are consistent with allochthonous organic carbon derived from freshwater sources and terrestrial C3 plants while marsh sediments located in the lower reaches are consistent with a high accumulation of marine phytoplankton and C4 marsh grasses (e.g. *Spartina* spp.). In the surface sediments of the RdlP, lower $\delta^{13}C$ values towards the upper reaches also indicated increasing deposition of terrestrial C3 plants, while towards the lower reaches the deposition events of marine algae would be more significant, with no carbon contribution of marsh grasses. Such a distributional pattern can clearly be related to the salinity gradient observed from the upper reaches to the middle estuary and the marine domain (Fig. 8), with a probable stronger influence of dissolved inorganic carbonates from freshwater which are characterized by low $\delta^{13}C$ in lower salinities (Fry and Sherr 1984). These results are consistent with previous studies suggesting that terrestrial organic matter is available as energy source for benthic consumers within the upper and middle reaches in the RdlP (Botto *et al.* 2011; Burone *et al.* 2013; Venturini *et al.* 2014; Marrero *et al.* 2014). Furthermore, our results are in agreement with recent findings showing that food sources including both estuarine microphytobenthos and diatoms show lower $\delta^{13}C$ values at low salinities rather than at high salinities (Lebreton *et al.* 2015).

Organic carbon sources in marsh core sediments

In our study, the $\delta^{13}C$ profiles obtained from the two marsh cores near the freshwater discharge (10-1 and 12-1) showed a decreasing trend from -24 to -28‰. Such depleted $\delta^{13}C$ values are indicative of a predominant freshwater source influence (with a typical range of -30 to -26‰,

322 Meyers 1994). Consistently, previous studies also attributed lower $\delta^{13}C$ values to stronger
323 influence of riverine particulate matter mostly composed of freshwater phytoplankton and C3
324 plant material with $\delta^{13}C$ values consistently between -29 and -26‰, that corresponded well with
325 those of the marsh cores from upper reaches of the RdlP (e.g. Wilson et al. 2005; Tue *et al.* 2011;
326 Lebreton *et al.* 2015). However, in the sediment cores from marshes adjacent to the lower
327 reaches of the RdlP (02-1, 08-1, 09-1, and 19-1) $\delta^{13}C$ values with a range from -9 to -19.5‰
328 reflect a considerably different composition of the organic matter. The remarkably low C/N
329 values in core 08-1 (<10) from the lower reaches confirmed a contribution of algal marine
330 sources in the sedimentary organic matter (Lamb *et al.* 2006). In addition, the $\delta^{13}C$ values of
331 *Spartina* spp. that dominates in marshes adjacent to the lower reaches of the RdlP showed values
332 around -11‰ (Botto *et al.* 2011), and therefore fall within the range of our $\delta^{13}C$ values registered
333 in marsh sediments from the lower reaches suggesting that C4 marsh grasses contribute to the
334 deposited sediment (autochthonous sediment deposition) together with marine organic matter
335 (allochthonous sediment deposition).
336
337 *Organic carbon sources in surface sediments within the RdlP*
338 In surface sediments along the RdlP, the progressive increase in $\delta^{13}C$ from the upper towards
339 lower reaches, with average values around -21‰, indicated a greater influence of ^{13}C-enriched
340 sources in the lower reaches of the estuary, including marine phytoplankton, and dissolved
341 inorganic carbon (Chanton and Lewis 1999). Furthermore, sedimentary C/N ratios were closer to
342 the ratios for marine phytoplankton, characterized by higher nitrogen-containing compounds
343 (C/N around 6-10; Meyers 1994; Lamb *et al.* 2006), thereby suggesting a lower contribution of
344 terrestrial derived organic matter in sediments from the lower reaches of the RdlP. This isotopic

pattern is opposed to the $\delta^{13}C$ values of -26 to -25‰ (i.e. in the range of terrestrial plant material and freshwater algae) found in the surface sediments from the upper reaches, indicating a contribution of terrestrial organic matter, and similar to what we found in the freshwater marshes. These results suggest that within the upper reaches of the RdlP river transports of organic matter are significantly contributing terrestrial derived material, including river POM, that represent a mixture of detritus and freshwater algae. This finding is consistent with the observation of Burone *et al.* (2013) who report an increased seaward marine influence in the transition zone of the RdlP. Previous studies in other estuaries also found a decreasing trend of $\delta^{13}C$ values in sediments from the lower reaches towards the upper reaches (Middelburg and Nieuwenhuize 1998; Zimmerman and Canuel 2001; Lautenschlager *et al.* 2014), indicating a higher contribution of ^{13}C-enriched marine sources to the allochthonous terrestrial sources towards the sea. The nMDS ordination analysis for isotope data and C/N ratios consistently grouped together samples from upper and lower reaches, while those of the middle reaches were dispersed into both groups. Furthermore, marsh vegetation seems not to influence adjacent coastal environments within the lower reaches of the RdlP dominated by marine derived organic matter. These results imply that most of the C4 marsh grasses (e.g. *Spartina* spp.) were processed within marsh habitats, and therefore act as a sink for organic carbon including marine phytoplankton.

Contribution of ENSO events to organic matter in core sediments

ENSO events influence the organic matter sources along the RdlP. Our $\delta^{13}C$ analysis in sediments from core 10-1, located in vicinity of the Paraná River, showed a generally decreasing trend towards present days, concurrent with an increase in the river discharge in the Paraná River

since the 1970s (Berbery *et al.* 2006; Marrero *et al.* 2014). Furthermore, in the sediment core 12-1, affected by the Uruguay River, abrupt changes in $\delta^{13}C$ values occurred in 2000/2001. This decreasing trend in $\delta^{13}C$ values together with C/N ratios showing distinct peaks higher than 10 during the strong ENSO events in the deposited organic matter supports the hypothesis that high periods of freshwater discharge that evolved during warm-phase ENSO events lead to an increased contribution of freshwater sources and terrestrial plant material. These results agree with findings of other studies that found evidence that the patterns of freshwater discharge and marine water intrusion moving in opposite direction control the dynamic energy of terrestrial subsidy and deposition to adjacent estuarine environments (Hoffman and Bronk 2006; Goñi *et al.* 2009; Hoeinghaus *et al.* 2011). Carbon sources from terrestrial organic matter, including invertebrates and autumn leaf fall, could have greater importance for aquatic ecosystems subsidizing aquatic organisms during high discharge periods (Junk *et al.* 1989). Furthermore, previous articles highlighted the important influence of ENSO events and river runoff patterns on fish assemblage (Garcia *et al.* 2001), on shrimp catches in the Patos Lagoon in southern Brazil (Moller *et al.* 2009), and also in ecosystem properties of the RdlP (Vögler *et al.* 2015). Our results (together with those of Schuerch *et al.* 2016) highlighted the effects of interannual climate variability linked to ENSO events, on the influence of the terrestrial/marine organic matter inputs drained into the RdlP estuary. Such a variability in organic matter composition may have significant implications on the production of species and food web structures. Furthermore, as a result of the higher inputs of nutrients and terrestrial organic matter during periods of high freshwater discharge, phytoplankton production may increase within the estuary, as reported by Machado et al. (2013), together with changes in the structure of the phytoplankton in coastal areas of the RdlP (Sathicq *et al.* 2015). In addition to the pattern of freshwater discharge, we

identified different variability of $\delta^{13}C$ values and C/N ratios among cores, which implied that the influence of marine vs. terrestrial organic matter was site specific. Local differences are likely caused by spatial difference in morphology, elevation, local hydrodynamics as well as the distance of the coring sites from the main channel, which impact the vegetation patterns, sources of organic matter and hence the variability in $\delta^{13}C$ values and C/N ratios (Isacch *et al.* 2006; Hoeinghaus *et al.* 2011). Furthermore, differences among cores may arise due to the inherent uncertainties (ca. ±3 years) of the radiocarbon dating (Schuerch *et al.* 2016).

Conclusions

Based on $\delta^{13}C$ values and C/N ratios we found that sources of organic matter in sediments within the RdlP can be separated into the upper, middle, and lower reaches. The RdlP estuary and adjacent marsh sites in the upper reaches received organic matter mostly from allochthonous sources (freshwater sources and C3 plant detritus), and autochthonous carbon sources tend to increase towards the lower reaches (marine algae). Additionally, our data suggested that marsh habitats did not supply sediments into the RdlP estuary, indicating minor erosion of marsh in the lower RdlP reaches. The marshes, therefore appear to act as a sediment sink, which has important implications for the marsh's function as sink for pollutants and nutrients in the estuary. Furthermore, extreme ENSO events tied with high freshwater discharge appear to play an important role in linking the terrestrial derived sources from adjacent habitats with the estuarine ecosystems. The information presented here is important to help infer and interpret similar processes of organic matter transport and composition in other large estuarine systems with distinct changes in continental terrigenous inputs.

Acknowledgements

We are grateful to the three anonymous referees for all the remarks and constructive comments that improved the manuscript. This work was partly funded by PEDECIBA-Geociencias and Agenica Nacional de Investigación en Innovación (SNI-ANII). This paper is part of the M.Sc. Thesis of A.T. This project (CP1211) was financially supported by a grant of the Cluster of Excellence 80 'The Future Ocean' to Mark Schuerch. 'The Future Ocean' is funded within the framework of the Excellence Initiative by the 'Deutsche Forschungsgemeinschaft' (DFG) on behalf of the German federal and state governments. L.B. thanks CSIC-Program 'Contratación de Científicos Provenientes del Exterior'.

References

Abrantes, K. G., Barnett A., Marwick T. R., and Bouillon, S. (2013). Importance of terrestrial subsidies for estuarine food webs in contrasting East African catchments. *Ecosphere* **4**, art14.

Abrantes, K., and Sheaves, M. (2008). Incorporation of terrestrial wetland material into aquatic food webs in a tropical estuarine wetland. *Estuarine, Coastal and Shelf Science* **80**, 401–412.

Appleby, P. G., and Oldfield, F. (1983). The assessment of ^{210}Pb data from sites with varying sediment accumulation rates. *Hydrobiologia* **103**, 29-35.

Barreiro, M. (2010). Influence of ENSO and the South Atlantic Ocean on climate predictability over Southeastern South America. *Climate Dynamics* **35**, 1493–1508.

437 Berbery, E., Doyle, M., and Barros, V. (2006). Regional Precipitation Trends, in: Barros, V.,
438 Clarke, R., Silva Dias, P.S., Climate Change in La Plata Basin. Trends in the Hydrological cycle
439 of the Plata basin, IAI-CONICET, Buenos Aires, pp. 61-73.
440
441 Bischoff, S. A., Garcia, N.O., Vargas, W. M., Jones, P. D., Conway, D. (2000). Climate
442 variability and Uruguay River flows. *Water International* **25**, 446–456.
443
444 Botto, F., Gaitán, E., Mianzan, H., Acha, M., Giberto, D., Schiariti, A., and Iribarne, O. (2011).
445 Origin of resources and trophic pathways in a large SW Atlantic estuary: an evaluation using
446 stable isotopes. *Estuarine Coastal and Shelf Science* **92**, 70–77.
447
448 Burone, L., Ortega, L., Franco-Fraguas, P., Mahiques, M., García-Rodriguez, F., Venturini, N.,
449 Marin, Y., Brugnoli, E., Nagai, R., Muniz, P., Bícego, M., Figueira, R., and Salaroli, A. (2013).
450 A multiproxy study between the Río de la Plata and the adjacent South-western Atlantic inner
451 shelf to assess the sediment footprint of river vs. marine influence. *Continental Shelf Research*
452 **55**,141–154.
453
454 Camilloni, I.A., and Barros, V.R. (2000). The Paraná River response to El Niño 1982–83 and
455 1997–98 events. *Journal of. Hydrometeorology* **1**, 412–430.
456
457 Calliari, D., Brugnoli, E., Ferrari, G., and Vizziano, D. (2009). Phytoplankton distribution and
458 production along a wide environmental gradient in the South-West Atlantic off Uruguay.
459 *Hidrobiologia* **620**, 47–61.

Calliari, D., Gómez, M., and Gómez, N. (2005). Biomass and composition of the phytoplankton in the Río de la Plata: large-scale distribution and relationship with environmental variables during a spring cruise. *Continental Shelf Research* **25**, 197–210.

Chanton, J., and Lewis, F. (1999). Plankton and dissolved inorganic carbon isotopic composition in a river-dominated estuary: Apalachicola Bay, Florida. *Estuaries* **22**, 575–583.

Cole, J. J., Carpenter, S.R., Kitchell, J., Pace, M. L., Solomon, C. T., and Weidel, B. (2011). Strong evidence for terrestrial support of zooplankton in small lakes based on stable isotopes of carbon, nitrogen, and hydrogen. *Proceeding of the National Academy of Sciences of the USA* **108**, 1975–1980.

Depetris, P. J., Kempe, S., Latif, M., and Mook, W. G. (1996). ENSO-controlled flooding in the Paraná River (1904–1991). *Naturwissenschaften* **83**, 127–129.

Framiñan, M., and Brown, O. (1996). Study of the Río de la Plata turbidity front, part 1: spatial and temporal distribution. *Continental Shelf Research* **16**, 1259–1282.

FREPLATA. (2004). Análisis Diagnóstico Transfronterizo del Río de la Plata y su Frente Marítimo. Documento Técnico Proyecto. Protección Ambiental del Río de la Plata y su Frente Marítimo: prevención y Control de la Contaminación y Restauración de Hábitats. Proyecto PNUD/GEF/RLA/99/G31.

Fry, B., and Sherr, E.B. (1984). $\delta^{13}C$ measurements as indicators of carbon flow in marine and freshwater ecosystems. *Contributions in Marine Science* **27**, 13–47.

Garcia, A.M., Vieira, J.P., and Winemiller, K. O. (2001). Dynamics of the shallow-water fish assemblage of the Patos Lagoon estuary (Brazil) during cold and warm ENSO episodes. *Journal of Fish Biology* **59**, 1218–1238.

García-Rodríguez, F., Brugnoli, E., Muniz, P., Venturini, N., Burone, L., Hutton, M., Rodríguez, M., Kandratavicius, N., Pérez, L., and Verocai, J. (2014). Warm phase ENSO events modulate the continental freshwater input and the trophic state of sediments in a large South American estuary. *Marine and Freshwater Research* **65**, 1-11.

Giberto, D. A., Bermec, C. A., Acha, E. M., and Mianzan, H. (2004). Large- scale spatial patterns of benthic assemblages in the SW Atlantic: the Rio de la Plata estuary and adjacent shelf waters. *Estuarine, Coastal and Shelf Science* **61**, 1–13.

Goñi, M. A., Voulgaris, G., and Kim, Y. H. (2009). Composition and fluxes of particulate organic matter in a temperate estuary (Winyah Bay, South Carolina, USA) under contrasting physical forcings. *Estuarine, Coastal and Shelf Science* **85**, 273–291.

Guerrero, R., Acha, E. M., Framiñan, M., and Lasta, C. (1997). Physical oceanography of the Rio de la Plata Estuary, Argentina. *Continental Shelf Research* **17**, 727–742.

Hammer, Ø., Harper, D. A. T., and Ryan, P. D. (2001). PAST: Paleontological Statistics Software Package for Education and Data Analysis. Palaeontologia Electronica 4(1): 9pp. http://palaeo-electronica.org/2001_1/past/issue1_01.htm

Hoeinghaus, D. J., Vieira, J. P., Costa, C. S., Bemvenuti, C. E., Winemiller, K. O., and Garcia A. M. (2011). Estuary hydrogeomorphology affects carbon sources supporting aquatic consumers within and among ecological guilds. *Hydrobiologia* **673**, 79–92.

Hoffman, J. C., and Bronk, D. A. (2006). Interannual variation in stable carbon and nitrogen isotope biogeochemistry of the Mettaponi River, Virginia. *Limnology and Oceanography* **51**, 2319–2332.

Isacch, J. P., Costa, C.S.B., Rodríguez-Gallego, L., Conde, D., Escapa, M., Gagliardini D.A., and Iribarne, O. O. (2006). Distribution of saltmarsh plat communities associated with environmental factors along a latitudinal gradient on the south-west Atlantic coast. *Journal of Biogeography* **33**, 888–900.

Junk, W. J., Bayley, P. B., and Sparks, R. E. (1989). The flood pulse concept in river–floodplain systems. Canadian Special Publication of Fisheries and Aquatic Sciences 106, 110–127.

Kruskal, J. B., and Wish, M. (1978). 'Multidimensional Scaling.' (Sage Publications: London.)

529 Lamb, A. L., Wilson G. P., and Leng, M. J. (2006). A review of coastal palaeoclimate and
530 relative sea-level reconstructions using $\delta^{13}C$ and C/N ratios in organic material. *Earth-Science*
531 *Reviews* **75**, 29–57.
532
533 Lautenschlager, A.D., Matthews, Ty G., and Quinn, G.P. (2014). Utilization of organic matter by
534 invertebrates along an estuarine gradient in an intermittently open estuary. *Estuarine, Coastal*
535 *and Shelf Science* **149**, 232–243.
536
537 Lebreton, B., Pollack, J.B., Blomberg, B., Palmer, T.A., Adams, L., Guillou, G., and Montagna,
538 P.A. (2015). Origin, composition and quality of suspended particulate organic matter in relation
539 to freshwater inflow in a South Texas estuary. *Estuarine, Coastal and Shelf Science* **170**, 70–82.
540
541 Machado, I., Barreiro, M., and Calliari, D. (2013). Variability of chlorophyll a in the Southwes-
542 tern Atlantic from satellite images: Seasonal cycle and ENSO influence. *Continental Shelf*
543 *Research* **53**, 102-109.
544
545 Malamud-Roam, F., and Ingram, B. L. (2001). Carbon isotopic compositions of plants and
546 sediments of tide marshes in the San Francisco Estuary. *Journal of Coastal Research* **17**, 17–29.
547
548 Marrero, A., Tudurí, A., Perez, L., Cuña, C., Muniz, P., Lopes Figueira, R.C., Michaelovitch de
549 Mahiques, M., Alves de Lima Ferreira, P., Pittauerová, D., Hanebuth, T., and García-Rodríguez,
550 F. (2014). Cambios históricos en el aporte terrígeno de la cuenca del Río de la Plata sobre la

plataforma interna uruguaya. *Latin American Journal of Sedimentology and Basin Analysis* **21**, 165–179.

Mechoso, C.R., and Perez-Iribarren, G. (1992). Streamflow in south-eastern South America and the Southern Oscillation. *Journal of Climate* **5**, 1535–1539.

Meyers, P. (1994). Preservation of elemental and isotopic source identification of sedimentary organic matter. *Chemical Geology* **114**, 289–302.

Meyers, P. (1997). Organic geochemical proxies of paleoceanographic, paleolimnologic, and paleoclimatic processes. *Organic geochemistry* **27**, 213–250.

Meyers, P. A. (2003). Applications of organic geochemistry to paleolimnological reconstructions: a summary of examples from the Laurentian Great Lakes. *Organic Geo-chemistry* **34**, 261–289.

Mianzan, H., Lasta, C., Acha, E., Guerrero, R., Macchi, G., and Bremec, C. (2001). The Río de la Plata estuary, Argentina-Uruguay. In: Seeliger, U., de Lacerda, L.D., Kjerve, B. (Eds.), Coastal Marine Ecosystems of Latin America. Springer-Verlag, Berlin, pp. 185–204.

Middelburg, J. J., and Nieuwenhuize, J. (1998). Carbon and nitrogen stable isotopes in suspended matter and sediments from the Schelde Estuary. *Marine Chemistry* **60**, 217-225.

574 Middelburg, J., Nieuwenhuize, J., Lubberts, R., and Vandeplassche, O. (1997). Organic carbon
575 isotope systematics of coastal marshes. *Estuarine, Coastal and Shelf Science* **45**, 681–687.
576
577 Möller, O. O., Castello, J.P., and Vaz, A.C. (2009). The effect of river discharge and winds on
578 the interannual variability of the pink shrimp *Farfantepenaeus paulensis* production in Patos
579 Lagoon. *Estuaries and Coasts* **32**, 787-796.
580
581 Müller, A., and Voss, M. (1999). The palaeoenvironments of coastal lagoons in the southern
582 Baltic Sea, - II. $\delta^{13}C$ and $\delta^{15}N$ ratios of organic matter - sources and sediments. *Palaeogeography*
583 *Palaeoclimatology Palaeoecology* **145**, 17–32.
584
585 Müller, P. J. (1977). C/N ratios in Pacific deep-sea sediments: Effect of inorganic ammonium
586 and organic nitrogen compounds sorbed by clays. Geochim. *Cosmochim. Acta* **41**, 765–776.
587
588 Nagy, G.J., Gómez-Erache, M., López, C.H., and Perdomo, A.C. (2002). Distribution patterns of
589 nutrients and symptoms of eutrophication in the Rio de la Plata estuary. *Hydrobiologia* **475**,
590 125–139.
591
592 Nakano, S., and Murakami, M. (2001). Reciprocal subsidies: dynamic interdependence between
593 terrestrial and aquatic food webs. *Proceeding of the National Academy of Sciences of the USA*,
594 **98**, 166–170.
595

Paerl, H. W. (2006). Assessing and managing nutrient-enhanced eutrophication in estuarine and coastal waters: interactive effects of human and climatic perturbations. *Ecological Engineering* **26**, 40–54.

Piola, A. R., Moller, O. O., Guerrero, R. A., and Campos, E. J. D. (2008). Variability of the subtropical shelf front off eastern South America: winter 2003 and summer 2004. *Continental Shelf Research* **28**, 1639–1648.

Polis, G. A., Anderson, W. B., and Holt, R. D. (1997). Toward an integration of landscape and food web ecology: the dynamics of spatially subsidized food webs. *Annual Review of Ecology and Systematics* **28**, 289–316.

Piovano, E., Ariztegui, D., Bernasconi, S. M. and McKenzie, J. A. (2004). Stable isotopic record of hydrological changes in subtropical Laguna Mar Chiquita (Argentina) over the last 230 years. *The Holocene* **14**, 525-535.

Remeikaitė-Nikienė, N., Lujanienė, G., Malejevas, V., Barisevičiūtė, R., Žilius, M., Garnaga-Budrė, G., and Stankevičius, A. (2016). Distribution and sources of organic matter in sediments of the south-eastern Baltic Sea. *Journal of Marine Systems* **157**, 75-81.

Sampei, Y., and Matsumoto, E. (2001). C/N ratios in a sediment core from Nakaumi Lagoon, southwest Japan. Usefulness as an organic source indicator. *Geochemical Journal* **35**, 189–201.

Sanchez-Cabeza, J. A., and Ruiz-Fernández, A. C. (2012). ^{210}Pb sediment radiochronology: An integrated formulation and classification of dating models. *Geochimica et Cosmochimica Acta* **82**, 183-200.

Sathicq, M. B., Bauer, D. E., and Gómez, N. (2015). Influence of El Niño Southern Oscillation phenomenon on coastal phytoplankton in a mixohaline ecosystem on the southeastern of South America: Río de la Plata estuary. *Marine Pollution Bulletin* **98**, 26–33.

Schuerch, M., Scholten, J., Carretero, S., García-Rodríguez, F., Kumbier, K., Baechtiger, M., and Liebetrau, V. (2016). The effect of long-term and decadal climate and hydrology variations on estuarine marsh dynamics: an identifying case study from the Río de la Plata. *Geomorphology* **269**, 122–132.

Tue, N. T., Hamaoka, H., Sogabe, A., Quy, T. D., Nhuan, M. T., and Omori, K. (2011). The application of δ^{13}C and C/N ratios as indicators of organic carbon sources and paleoenvironmental change of the mangrove ecosystem from Ba Lat Estuary, Red River, Vietnam. *Environmental Earth Sciences* **64**, 1475–1486.

Thornton, S. F., and McManus, J. (1994). Application of organic carbon and nitrogen stable isotope and C/N ratios as source indicators of organic matter provenance in estuarine systems: evidence from the Tay estuary, Scotland. *Estuarine, Coastal and Shelf Science* **38**, 219-233.

Valiela, I., and Bartholomew, M. (2015). Land–Sea coupling and global-driven forcing: following some of Scott Nixon's challenges. *Estuaries and Coasts* **38**, 1189–1201.

Venturini, N., Bícego M. C., Taniguchi, S., Sasaki, S. T., García-Rodríguez, F., Brugnoli E., and Muniz, P. (2014). A multi-molecular marker assessment of organic pollution in shore sediments from the Río de la Plata Estuary, SW Atlantic. *Marine Pollution Bulletin* **91**, 461–475.

Vögler, R., Arreguín-Sánchez, F., Lercari, D., del Monte-Luna, P., and Calliari, D. (2015). The effects of long-term climate variability on the trophodynamics of an estuarine ecosystem in southern South America. *Ecological Modelling* **317**, 83–92.

Werner, R. A., Bruch, B. A., and Brand, W.A. (1999). ConFlo III—an interface for high precision $\delta^{13}C$ and $\delta^{15}N$ analysis with an extended dynamic range. *Rapid Communications in Mass Spectrometry* **13**, 1237–1241.

Whitfield, A. K., and Elliott, M., 2011. Ecosystem and biotic classifications of estuaries and coasts, (Chapter 1) 8; In: Wolanski, E., McLusky, D.S. (Eds), Treatise on Estuaries and Coasts, Elsevier, Amsterdam.

Zimmerman, A. R., and Canuel, E. A. (2001). Bulk organic matter and lipid biomarker composition of Chesapeake Bay surficial sediments as indicators of environmental processes. *Estuarine, Coastal and Shelf Science* **53**, 319–341.

664 **FIGURE CAPTIONS**

665

666 **Fig. 1.** Map of the RdlP estuary and location of all sample sites. The station codes describe the
667 name of each site. Black stars indicate the location of the six marsh cores. Triangles and circles
668 indicate the location of the surface samples along the estuary with 24 sampling stations; white
669 circles: upper reaches; black triangles: middle reaches; and grey circles: lower reaches. Dashed
670 line represent a submersed bar (Barra del Indio shoal). Study period from March to June 2010.

671

672 **Fig. 2.** Standardized discharge in the Paraná and Uruguay rivers below and above the mean
673 estimated annual river discharge (m^3/s). Strong ENSO events (ONI indices > 1.5) are indicated
674 using triangles.

675

676 **Fig. 3.** $\delta^{13}C$ values and C/N ratios of sedimented organic matter versus age at two different
677 saltmarsh areas located in the upper reaches of the RdlP estuary (cores 12-1 and 10-1). ENSO
678 events are indicated using triangles on the y-axes. Core sites are indicated in Fig. 1.

679

680

681 **Fig. 4.** $\delta^{13}C$ values and C/N ratios of sedimented organic matter versus age at four different
682 saltmarsh areas located in the lower reaches of the RdlP estuary (cores 19-1, 08-1, 09-1 and 02-
683 1). ENSO events are indicated using triangles on the y-axes. Note that the y-axis of the plot for
684 the core 09-1 indicates depth in the sediments of the marsh core. Note also the different y-axis
685 scales. Core sites are indicated in Figure 1 Cores 19-1 and 02-1 presented no clear pattern in N

686 values that contribute with imprecision to infer organic matter sources; consequently C/N data
687 was judge unreliable and not further considered.
688
689 **Fig. 5.** Relationship between $\delta^{13}C$ and C/N values of the sediments from the saltmarshes habitats
690 located in the upper (10-1 and 12-1) and lower reaches (09-1, 08-1, 19-1 and 02-1) of the RdlP,
691 including typical ranges of sources according to data presented by Meyers (1994) and Lamb *et*
692 *al.* (2006). Core sites are indicated in Figure 1. Cores 19-1 and 02-1 presented no clear pattern in
693 N values that contribute with imprecision to infer organic matter sources; consequently C/N data
694 was judge unreliable and not further considered.
695
696 **Fig. 6.** Relationship between $\delta^{13}C$ and C/N values of the surface sediments from each sampling
697 station within the RdlP estuary (upper, middle and lower reaches) in March (warm season) and
698 June (cold season) 2010, including typical ranges of sources according to data presented by
699 Meyers (1994) and Lamb et al. (2006).
700
701 **Fig. 7.** Two-dimensional nMDS ordination of the C/N ratios and isotopic composition of
702 sediments from the upper (U), middle (M) and lower reaches (L) within the RdlP estuary (a) and
703 adjacent marsh sites (b). The data are standardized and the matrix was performed using
704 normalized Euclidian distances. For the marsh cores we include all dates in the analysis.
705
706 **Fig. 8.** Carbon stable isotopes $\delta^{13}C$ (‰) of surface sediments versus salinities of each sampling
707 stations within the Río de la Plata estuary at both sampling dates: grey filled circle lower reaches,
708 black triangles middle reaches, and open circle upper reaches.

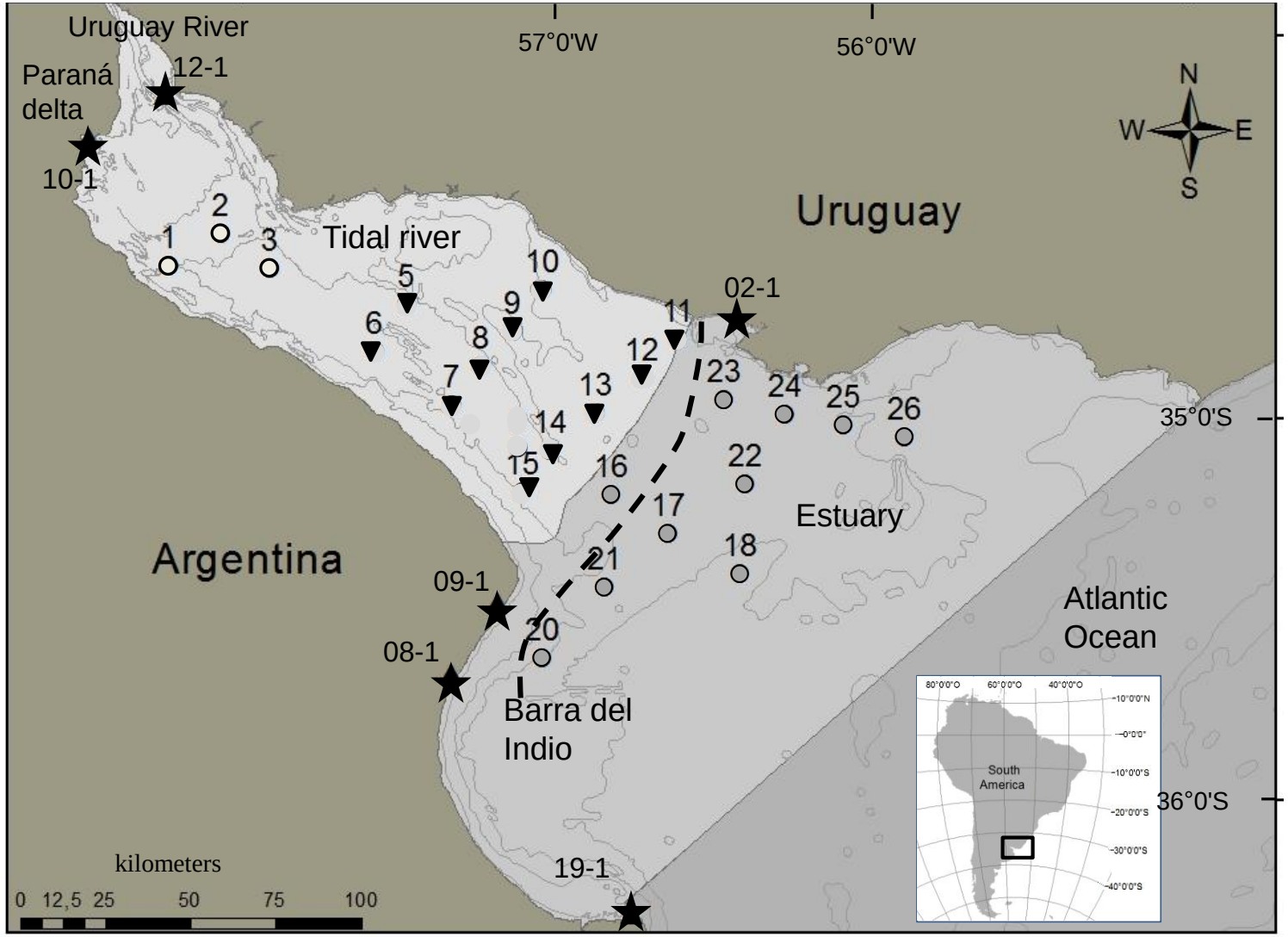
Uruguay River
Paraná
delta
12-1
10-1
57°0'W
56°0'W
N
W
E
S
Uruguay
Tidal river
1
2
3
5
6
7
8
9
10
11
12
13
14
15
16
17
18
21
02-1
23
24
25
26
22
35°0'S
Estuary
Argentina
09-1
08-1
20
Barra del
Indio
Atlantic
Ocean
19-1
36°0'S
kilometers
0 12,5 25 50 75 100
South
America

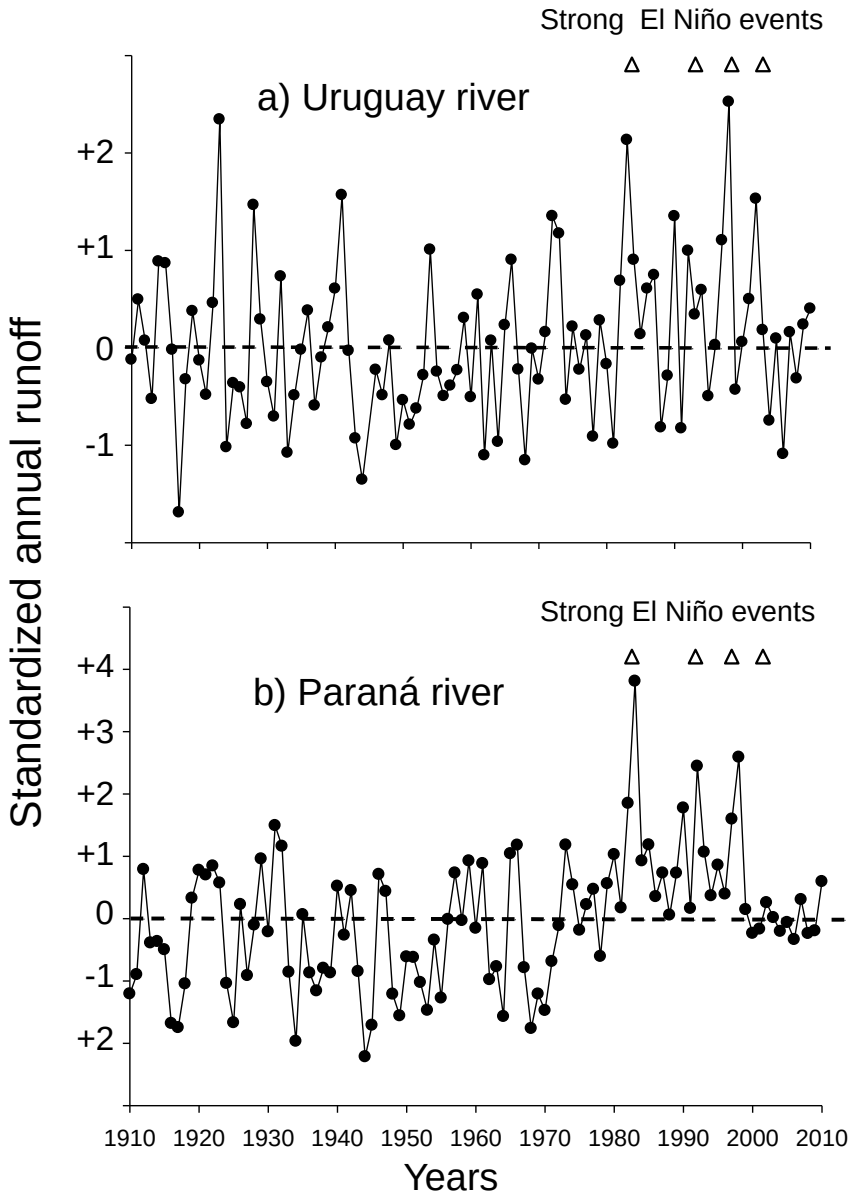
Strong El Niño events
a) Uruguay river
+2
+1
0
-1
Strong El Niño events
b) Paraná river
+4
+3
+2
+1
0
-1
+2
Standardized annual runoff
1910
1920
1930
1940
1950
1960
1970
1980
1990
2000
2010
Years

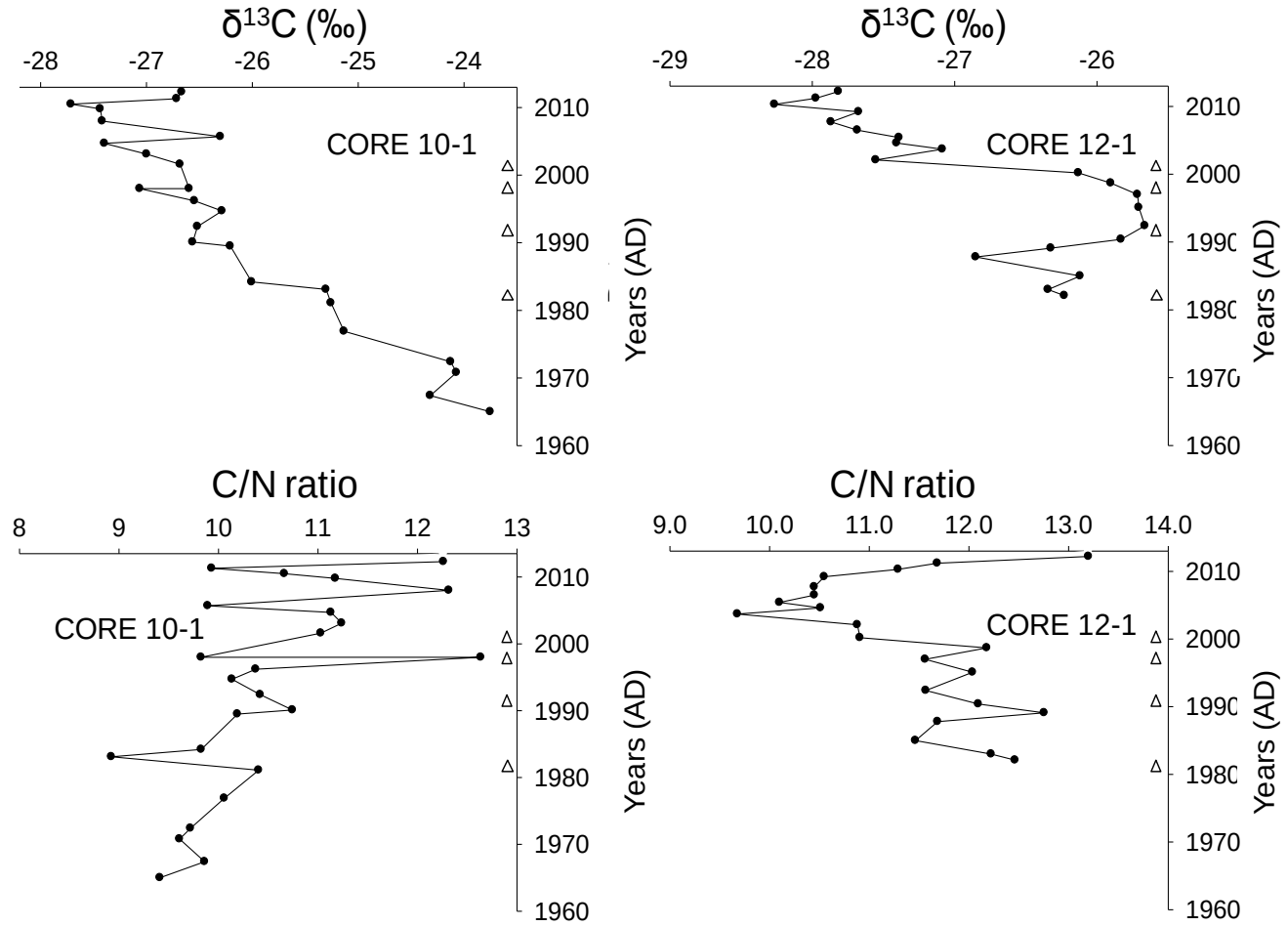
δ13C (‰)
-28
-27
-26
-25
-24
CORE 10-1
2010
2000
1990
1980
1970
1960
Years (AD)
δ13C (‰)
-29
-28
-27
-26
CORE 12-1
2010
2000
1990
1980
1970
1960
Years (AD)
C/N ratio
8
9
10
11
12
13
CORE 10-1
2010
2000
1990
1980
1970
1960
Years (AD)
C/N ratio
9.0
10.0
11.0
12.0
13.0
14.0
CORE 12-1
2010
2000
1990
1980
1970
1960
Years (AD)

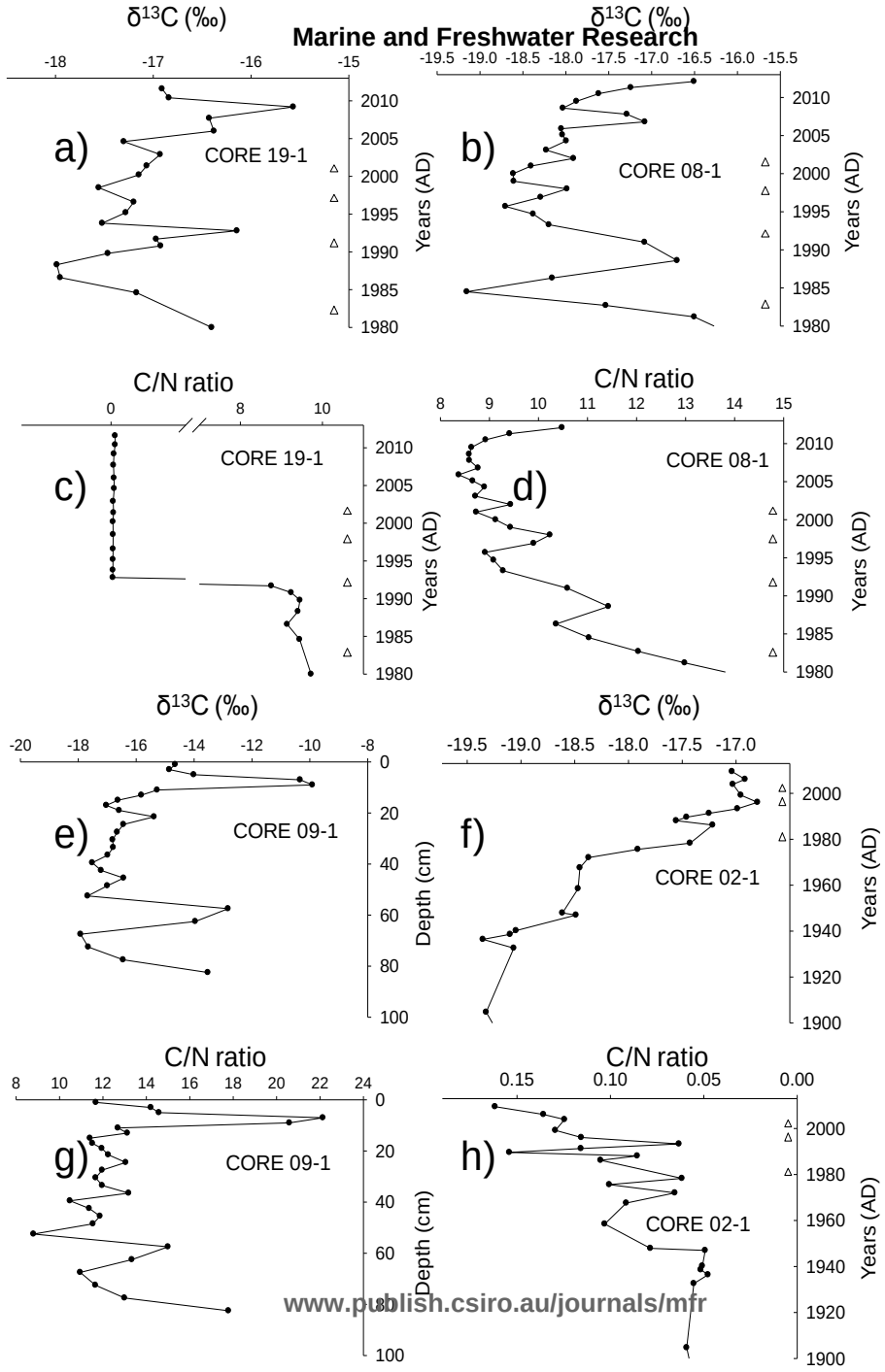
δ13C (‰)
a)
CORE 19-1
Years (AD)
δ13C (‰)
b)
CORE 08-1
Years (AD)
C/N ratio
c)
CORE 19-1
Years (AD)
C/N ratio
d)
CORE 08-1
Years (AD)
δ13C (‰)
e)
CORE 09-1
Depth (cm)
δ13C (‰)
f)
CORE 02-1
Years (AD)
C/N ratio
g)
CORE 09-1
Depth (cm)
C/N ratio
h)
CORE 02-1
Years (AD)

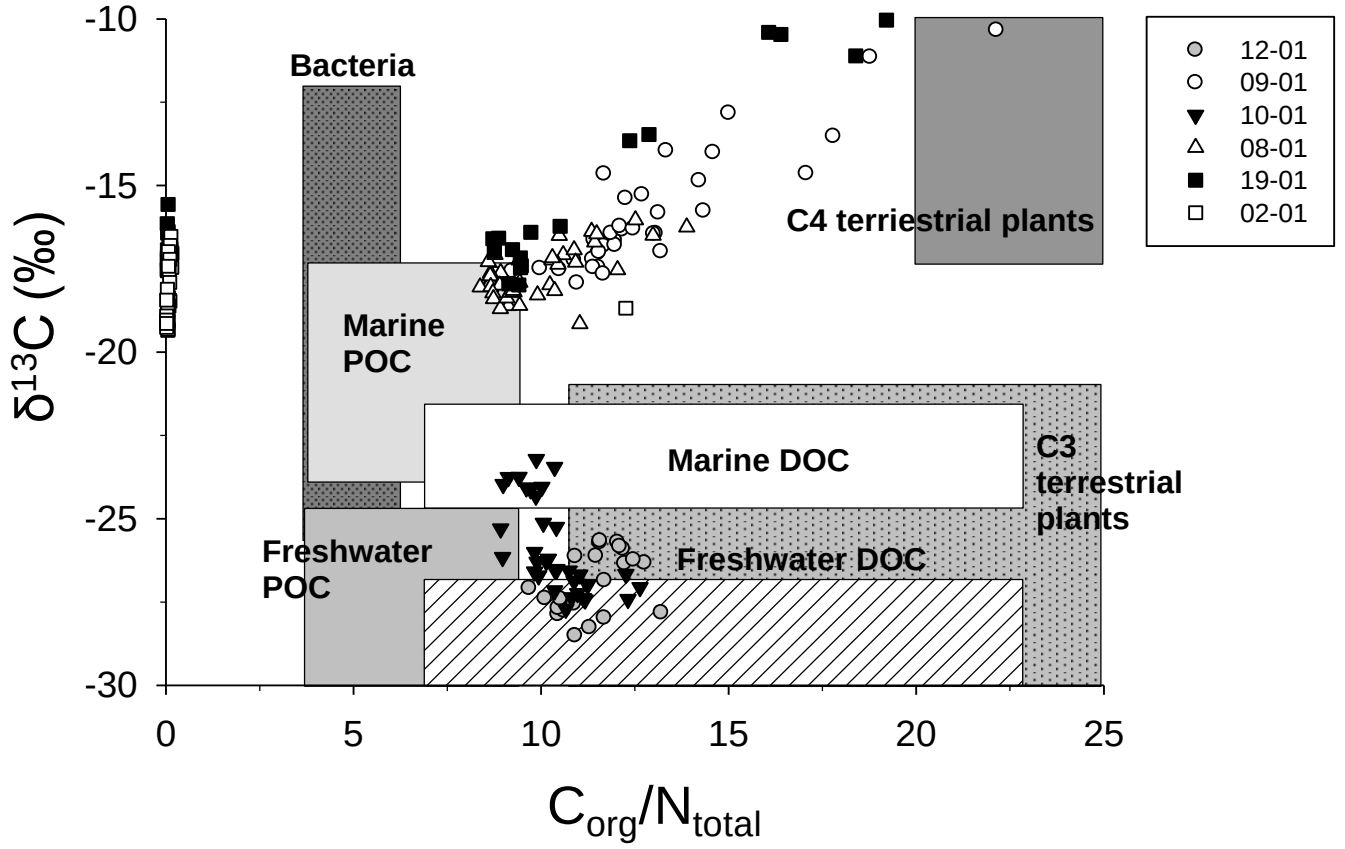
-10
-15
-20
-25
-30
0
5
10
15
20
25
δ13C (‰)
Corg/Ntotal
Bacteria
Marine POC
Marine DOC
C4 terriestrial plants
C3 terrestrial plants
Freshwater POC
Freshwater DOC
12-01
09-01
10-01
08-01
19-01
02-01

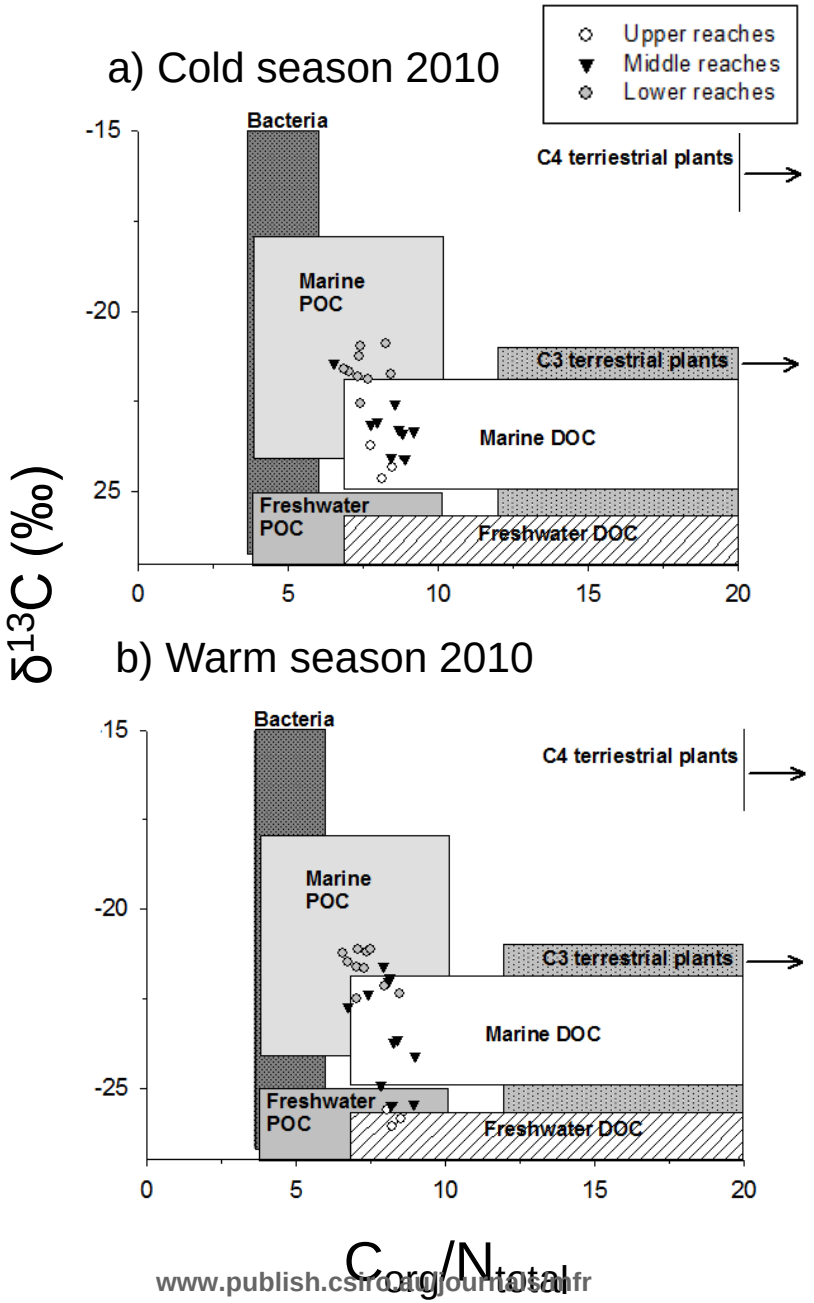

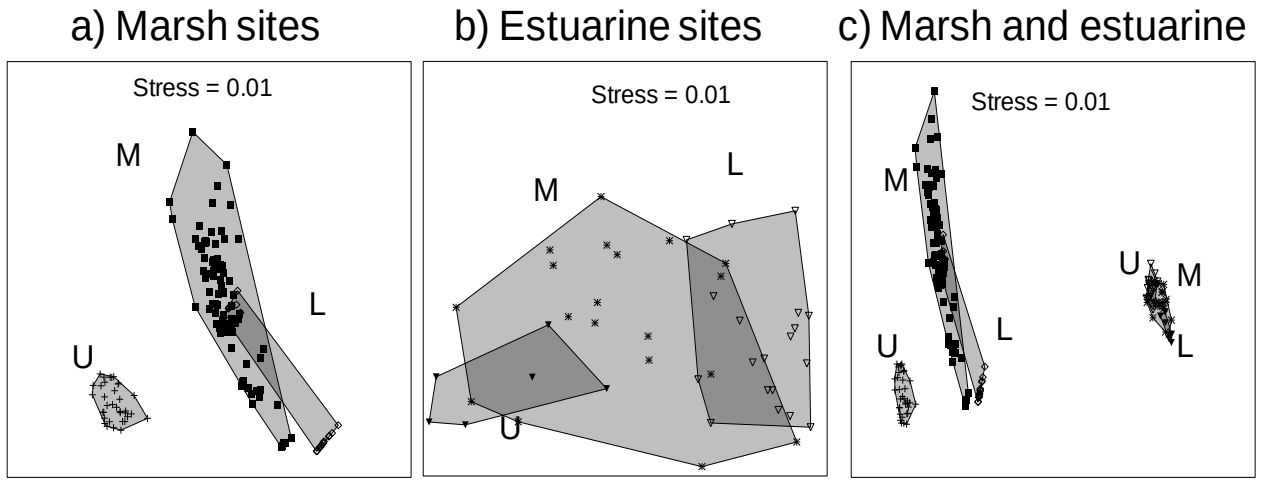
a) Marsh sites
Stress = 0.01
M
L
U
b) Estuarine sites
Stress = 0.01
M
L
U
c) Marsh and estuarine
Stress = 0.01
M
L
U
U
M
L

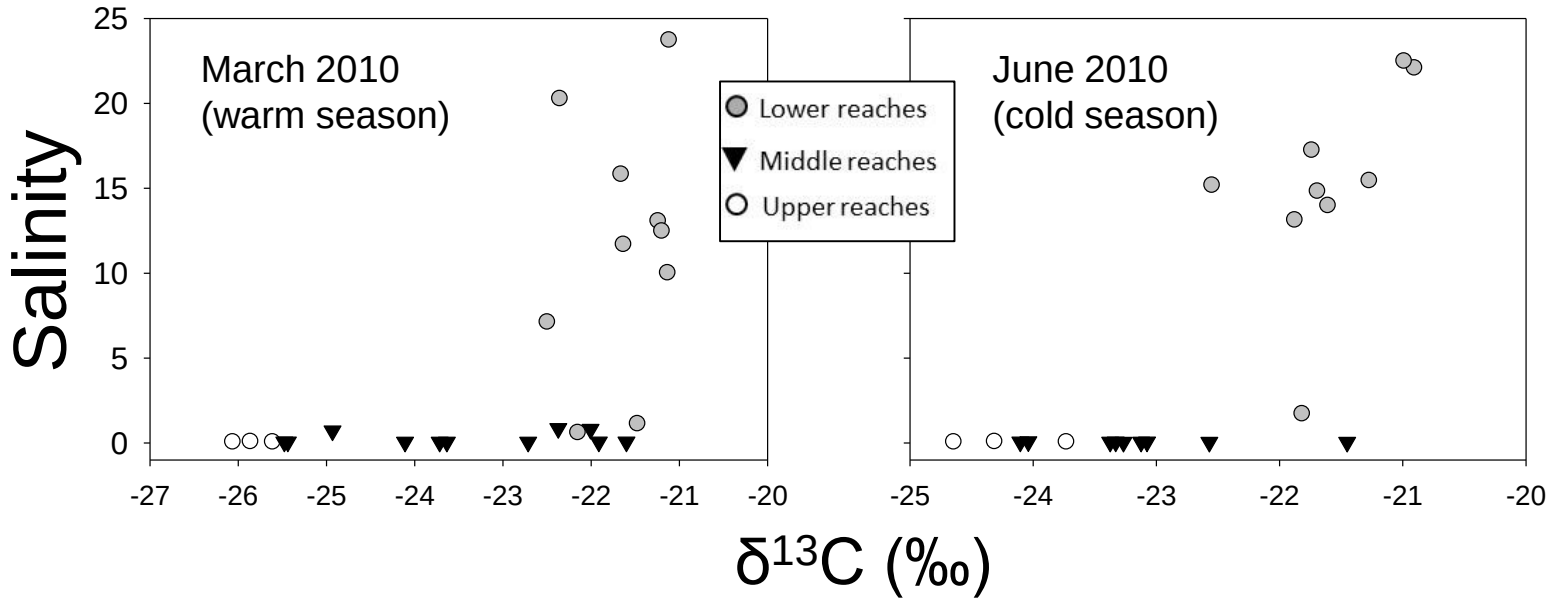
March 2010
(warm season)
June 2010
(cold season)
Lower reaches
Middle reaches
Upper reaches
Salinity
δ13C (‰)
25
20
15
10
5
0
-27
-26
-25
-24
-23
-22
-21
-20
-25
-24
-23
-22
-21
-20

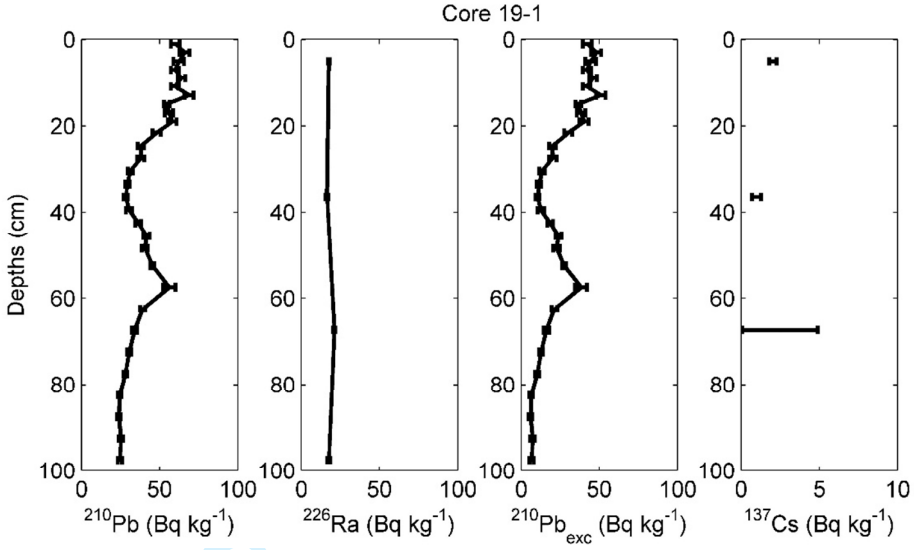

Figure S1: Raw data of radionuclide measurements in core 19-1.

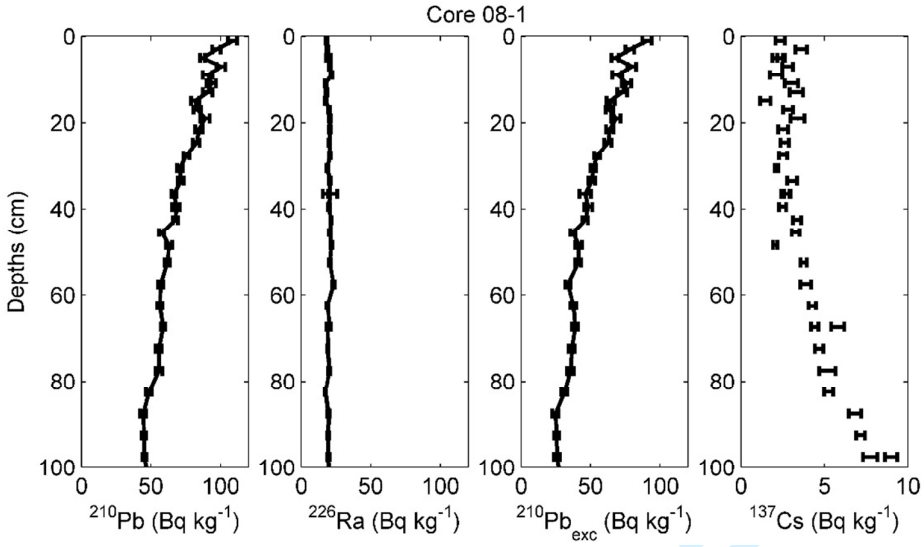

Figure S2: Raw data of radionuclide measurements in core 08-1.

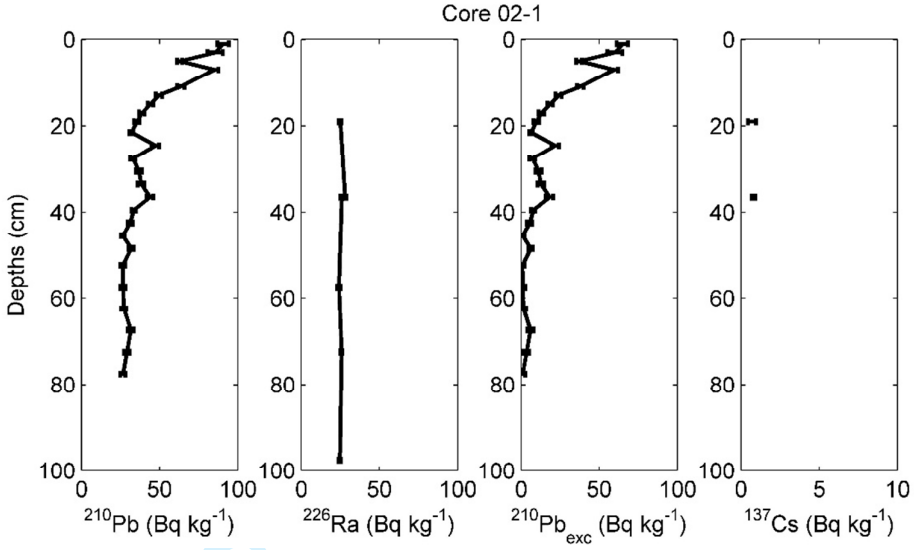

Figure S3: Raw data of radionuclide measurements in core 02-1.

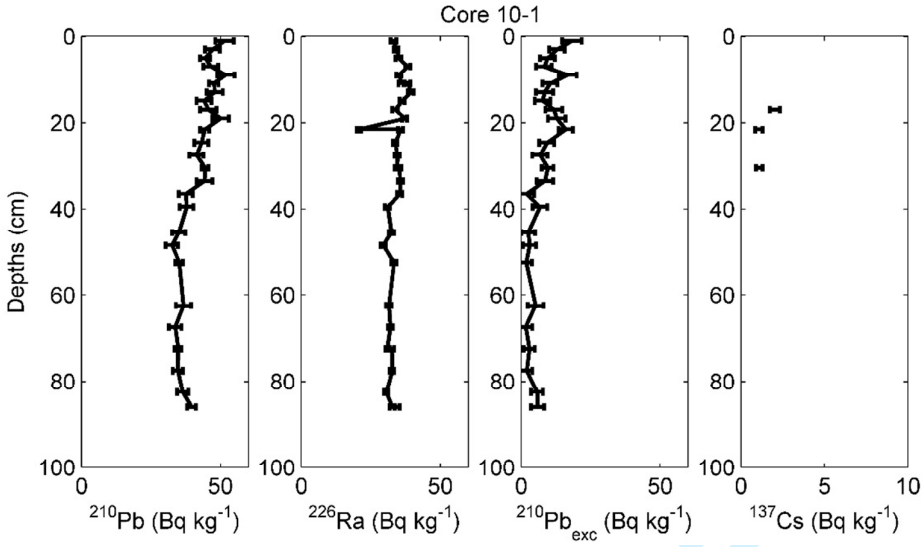

Figure S4: Raw data of radionuclide measurements in core 10-1.

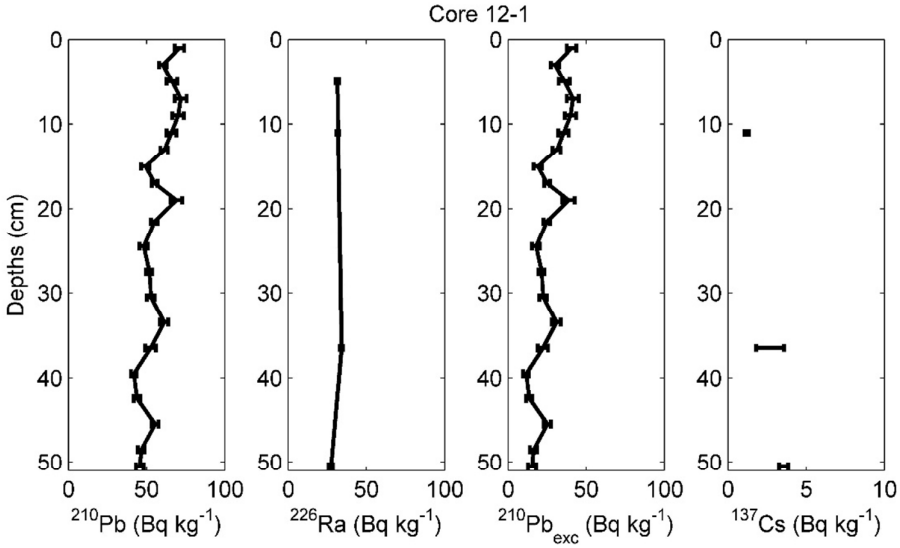

Figure S5: Raw data of radionuclide measurements in core 12-1.

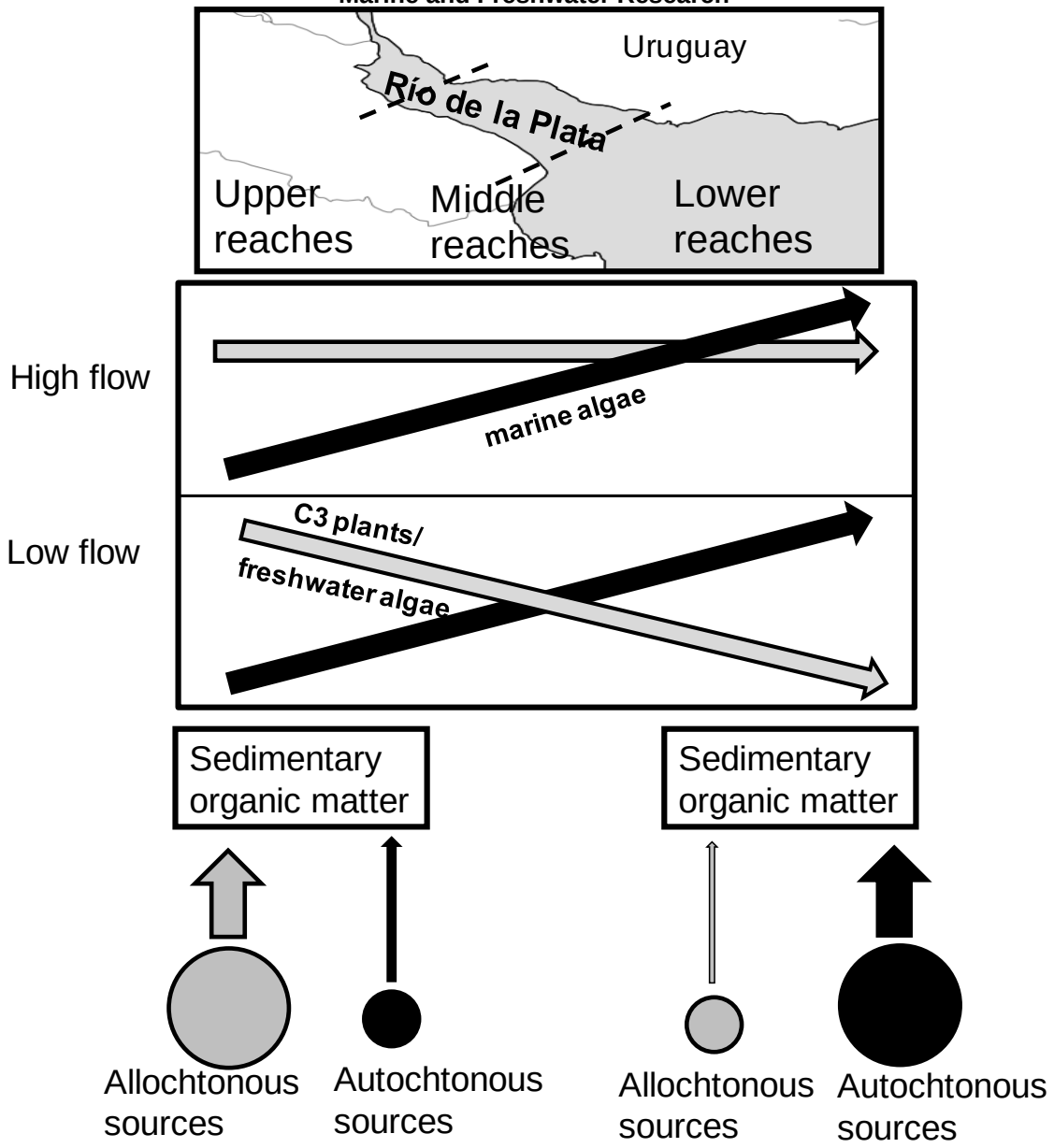
Uruguay
Río de la Plata
Upper reaches
Middle reaches
Lower reaches
High flow
marine algae
Low flow
C3 plants/
freshwater algae
Sedimentary organic matter
Sedimentary organic matter
Allochtonous sources
Autochtonous sources
Allochtonous sources
Autochtonous sources